Tsc/mTORC1 signaling in oocytes governs the quiescence and activation of primordial follicles

Deepak Adhikari[1], Wenjing Zheng[1], Yan Shen[1], Nagaraju Gorre[1], Tuula Hämäläinen[2], Austin J. Cooney[3], Ilpo Huhtaniemi[2,4], Zi-Jian Lan[5] and Kui Liu[1,*]

[1]Department of Medical Biochemistry and Biophysics, Umeå University, Umeå SE-901 87, Sweden, [2]Department of Physiology, Institute of Biomedicine, University of Turku, Turku 20520, Finland, [3]Department of Molecular and Cellular Biology, Baylor College of Medicine, Houston, TX 77030, USA, [4]Department of Reproductive Biology, Imperial College London, Hammersmith Campus, London W12 0NN, UK and [5]Birth Defects Center, Department of Molecular, Cellular and Craniofacial Biology, University of Louisville Health Sciences Center, Louisville, KY 40202, USA

To maintain the female reproductive lifespan, the majority of ovarian primordial follicles are preserved in a quiescent state in order to provide ova for later reproductive life. However, the molecular mechanism that maintains the long quiescence of primordial follicles is poorly understood. Here we provide genetic evidence to show that the tumor suppressor tuberous sclerosis complex 1 (Tsc1), which negatively regulates mammalian target of rapamycin complex 1 (mTORC1), functions in oocytes to maintain the quiescence of primordial follicles. In mutant mice lacking the *Tsc1* gene in oocytes, the entire pool of primordial follicles is activated prematurely due to elevated mTORC1 activity in the oocyte, ending up with follicular depletion in early adulthood and causing premature ovarian failure (POF). We further show that maintenance of the quiescence of primordial follicles requires synergistic, collaborative functioning of both Tsc and PTEN (phosphatase and tensin homolog deleted on chromosome 10) and that these two molecules suppress follicular activation through distinct ways. Our results suggest that Tsc/mTORC1 signaling and PTEN/PI3K (phosphatidylinositol 3 kinase) signaling synergistically regulate the dormancy and activation of primordial follicles, and together ensure the proper length of female reproductive life. Deregulation of these signaling pathways in oocytes results in pathological conditions of the ovary, including POF and infertility.

INTRODUCTION

In the mammalian ovary, the pool of primordial follicles is the source of ova for the entire reproductive life. To maintain the normal length of female reproductive life, the majority of primordial follicles must be maintained in a quiescent state for later use (1–3). In order to produce mature ova, primordial follicles are recruited from the reservoir of dormant follicles into the growing follicular pool, through a process termed follicular activation or initial recruitment, and subsequently undergo a series of follicular development (2). Menopause, or ovarian senescence, occurs when the pool of primordial follicles has become exhausted (4–6).

Investigation of the molecular mechanisms that sustain the long dormancy of primordial follicles is still in its infancy (7). Recently, our studies revealed that PTEN (phosphatase and tensin homolog deleted on chromosome 10), a negative regulator of PI3K (phosphatidylinositol 3 kinase), functions in oocytes as a suppressor of follicular activation (8). We also found that the PI3K–PDK1 (3-phosphoinositide-dependent protein kinase-1)–Akt–S6K1 (p70 S6 kinase 1)–rpS6 (ribosomal protein S6) cascade in primary oocytes regulates ovarian aging by regulating the survival of primordial follicles (9). These results indicate that PTEN/PI3K signaling within the oocyte is of importance in determining the developmental courses of the primordial follicles, including their survival, their activation and their demise.

*To whom correspondence should be addressed. Tel. +1 46 907867762; Fax: +1 46907865450, E-mail: kui.liu@medchem.umu.se

It is worthwhile noting that in wild-type and *Pten*-deficient oocytes, the activation of S6K1–rpS6 is largely dependent on mammalian target of rapamycin complex 1 (mTORC1) (8), indicating that mTOR signaling may be a regulatory network associated with control of the development of primordial follicles.

mTORC1 is a serine/threonine kinase that regulates cell growth and proliferation in response to growth factors and nutrients. It functions by modulating processes such as protein synthesis, ribosome biogenesis and autophagy (10–12). In human cells, mTORC1 activity is negatively regulated by a heterodimeric complex consisting of two protein molecules: tuberous sclerosis complex 1 (TSC1 or hamartin) and TSC2 (or tuberin). TSC1 and TSC2 are products of two distinct tumor suppressor genes: *TSC1* and *TSC2*, respectively. These two genes are the genetic loci that are mutated in the autosomal dominant tumor syndrome tuberous sclerosis complex (TSC), which is characterized by numerous benign tumors (13–15). The TSC1–TSC2 complex suppresses the activation of mTORC1 through a GTPase activating protein domain located in TSC2. The function of TSC1 is to stabilize TSC2 and protect it from ubiquitination and degradation (16).

Mouse models with conventional deletion of *Tsc1* or *Tsc2* exhibit embryonic lethality, making them difficult to use to study the functional roles of Tsc/mTORC1 signaling in a specific organ (14,17). To determine whether the Tsc/mTORC1 signaling in oocytes takes part in regulation of the development of primordial follicles, in this study, we deleted the *Tsc1* gene from mouse oocytes in primordial and further developed follicles. Deletion of *Tsc1* led to a global activation of all primordial follicles around the time of puberty, ending up with follicular depletion in early adulthood and causing premature ovarian failure (POF). Thus, the Tsc1–Tsc2 complex in mouse oocytes is indispensable for sustaining the dormant state of primordial follicles. Moreover, our results also revealed that Tsc and PTEN synergistically maintain the dormancy of primordial follicles: both through suppression of S6K1 activity, but by downregulation of S6K1 phosphorylation at distinct sites, i.e. threonine 389 (T389) and T299, respectively. Thus, collaborative functioning of Tsc and PTEN is required to maintain the quiescence of primordial follicles, which is in turn required to preserve the length of female reproductive life.

RESULTS

Generation of mutant mice with oocyte-specific deletion of *Tsc1*

To study how the Tsc1–Tsc2 complex in oocytes controls the development of primordial follicles, we generated mutant mice in which the *Tsc1* gene was deleted in oocytes of primordial and further developed follicles (referred to as Oo*Tsc1*$^{-/-}$ mice). This was achieved by crossing *Tsc1*$^{loxP/loxP}$ mice (14) with transgenic mice expressing *growth differentiation factor 9* (*Gdf-9*) promoter-mediated Cre recombinase (18) (Fig. 1A). By western blot, we found that expression of Tsc1 (hamartin) protein was completely absent in growing Oo*Tsc1*$^{-/-}$ oocytes (Fig. 1B), indicating successful deletion of the *Tsc1* gene from oocytes.

We found that the Oo*Tsc1*$^{-/-}$ females had a normal vaginal opening at the age of 5–6 weeks (which is the appropriate
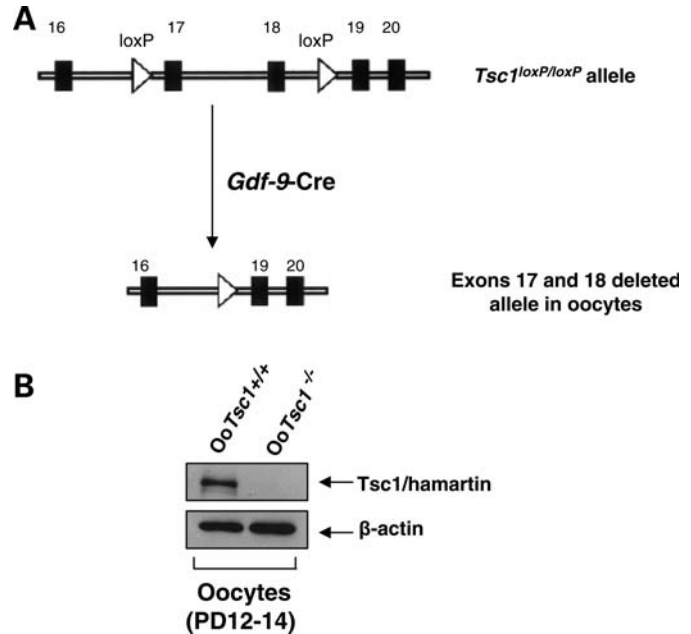

Figure 1. Oocyte-specific deletion of *Tsc1* in mice. (**A**) Schematic representation of deletion of *Tsc1* exons 17 and 18 by *Gdf-9*-Cre-mediated recombination in oocytes. (**B**) Western blots showing the absence of Tsc1 (hamartin) protein expression in oocytes of Oo*Tsc1*$^{-/-}$ mice. Oocytes were isolated from ovaries of 12- to 14-day-old Oo*Tsc1*$^{+/+}$ and Oo*Tsc1*$^{-/-}$ mice as described in Materials and Methods. For each experiment, material from 3–5 mice was used per lane. For each lane, ~20 μg of protein was loaded. Levels of β-actin were used as internal controls. The experiments were repeated three times and representative images are shown.

age). However, during the period from 6 to 27 weeks of age, the Oo*Tsc1*$^{-/-}$ females were found to produce at most 2 litters of normal size, but then became infertile in young adulthood (i.e. after 12–13 weeks of age) (Fig. 2).

Premature activation of the entire pool of primordial follicles in Oo*Tsc1*$^{-/-}$ mice

To determine how the loss of *Tsc1* from oocytes impedes mouse fertility, we compared the first wave of postnatal follicular development in Oo*Tsc1*$^{-/-}$ mice to that in Oo*Tsc1*$^{+/+}$ mice. No apparent morphological difference was found in post-natal day (PD) 5 ovaries of Oo*Tsc1*$^{-/-}$ and Oo*Tsc1*$^{+/+}$ mice, where ovaries of both genotypes had mostly primordial and some primary follicles (Fig. 3A–C). By PD23, however, the Oo*Tsc1*$^{-/-}$ ovaries (Fig. 3E) appeared larger than the Oo*Tsc1*$^{+/+}$ ovaries (Fig. 3D). All primordial follicles were activated in Oo*Tsc1*$^{-/-}$ ovaries with enlarged oocytes (Fig. 3F, arrows; Fig. 3H), whereas 74% of the follicles in control ovaries were still at the primordial stage (Fig. 3D, arrows; Fig. 3H). This leads to higher numbers of activated follicles in Oo*Tsc1*$^{-/-}$ ovaries (Fig. 3H, Acti). There were also more follicles in Oo*Tsc1*$^{-/-}$ ovaries at PD23 (Fig. 3H), including transient follicles containing enlarged oocytes surrounded by flattened pregranulosa cells (Fig. 3F, arrows), and type 4 and type 5 follicles (Fig. 3H). Thus, with *Tsc1* deleted in oocytes, the entire pool of primordial follicles in Oo*Tsc1*$^{-/-}$ ovaries had been activated by
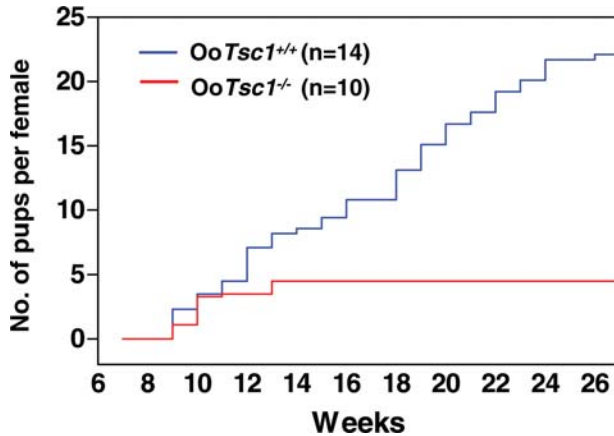
Figure 2. Subfertility in mice upon deletion of *Tsc1* from oocytes. Comparison of the cumulative number of pups per Oo*Tsc1*$^{-/-}$ female ($n = 10$, red line) and per Oo*Tsc1*$^{+/+}$ female ($n = 14$, blue line). All Oo*Tsc1*$^{-/-}$ females became infertile in young adulthood after week 12–13.

PD23, and the post-natal follicular loss that usually takes place before the onset of sexual maturity (19,20) had also been prevented to some extent.

Follicle depletion and POF in early adulthood in Oo*Tsc1*$^{-/-}$ mice

By 7 weeks of age, the Oo*Tsc1*$^{-/-}$ ovaries (Fig. 4B) still appeared larger than the Oo*Tsc1*$^{+/+}$ ovaries (Fig. 4A), due to higher numbers of activated follicles (Fig. 4J). However, some of the prematurely activated follicles (especially the transient follicles with enlarged oocytes) had started to degenerate (Fig. 4C, arrows); thus, the total numbers of follicles in Oo*Tsc1*$^{-/-}$ ovaries had become less than in Oo*Tsc1*$^{+/+}$ ovaries at this age (Fig. 4J).

By 2 months of age, the Oo*Tsc1*$^{-/-}$ ovaries (Fig. 4E) appeared smaller than Oo*Tsc1*$^{+/+}$ ovaries (Fig. 4D) because most of the follicles had been degraded (Fig. 4F, arrows), and the numbers of healthy follicles were less than those in Oo*Tsc1*$^{+/+}$ ovaries (Fig. 4D). Ovulation had taken place in Oo*Tsc1*$^{-/-}$ ovaries, as indicated by the presence of corpora lutea (CL) (Fig. 4E, arrow). By 3 months of age, Oo*Tsc1*$^{-/-}$ ovaries were smaller and did not have any healthy follicular structure (Fig. 4H and I). As a control, the Oo*Tsc1*$^{+/+}$ ovaries were larger, showing healthy follicles and CL (Fig. 4G). These results indicate that POF had already taken place in 2- to 3-month-old Oo*Tsc1*$^{-/-}$ mice. In addition, in sera of 3- to 4-month-old Oo*Tsc1*$^{-/-}$ mice, the levels of follicle-stimulating hormone (FSH) (Fig. 4K) and luteinizing hormone (LH) (Fig. 4L) were significantly higher when compared with age-matched Oo*Tsc1*$^{+/+}$ mice. Thus, premature activation of the primordial follicle pool led to follicle depletion and POF in Oo*Tsc1*$^{-/-}$ mice in early adulthood.

Enhanced mTORC1 activity in Oo*Tsc1*$^{-/-}$ oocytes

To elucidate the molecular mechanisms underlying the accelerated oocyte growth in Oo*Tsc1*$^{-/-}$ ovaries, we studied the signaling molecules that are regulated by Tsc in

Oo*Tsc1*$^{-/-}$ oocytes. First of all, we found that in the absence of Tsc1, Tsc2 was also absent in Oo*Tsc1*$^{-/-}$ oocytes (Fig. 5A), confirming that the function of Tsc1 is to stabilize Tsc2 (16) in oocytes.

mTOR is associated with two distinct complexes, mTORC1 and mTOR complex 2 (mTORC2) (21,22). mTORC1 is rapamycin-sensitive (23) and promotes cell growth largely through activation of S6K1 (by phosphorylation of its threonine 389) and through phosphorylation and inactivation of eukaryotic translation initiation factor 4E (eIF4E)-binding proteins (4E-BPs) (12,24). S6K1 is responsible for phosphorylation and activation of rpS6, which leads to enhanced protein translation and ribosome biogenesis (12). 4E-BP1 represses the activity of eIF4E, and phosphorylation of 4E-BP1 by mTORC1 releases its suppression of eIF4E and promotes protein translation (25). In contrast, mTORC2 is rapamycin-insensitive and has been shown to phosphorylate Akt at its serine 473 (S473) (11).

We found that in Oo*Tsc1*$^{-/-}$ oocytes the activity of mTORC1 was enhanced, as indicated by the elevated levels of phosphorylated S6K1 (Fig. 5A, p-S6K1, T389) and phosphorylated 4E-BP1 (Fig. 5A, p-4E-BP1, S65) in Oo*Tsc1*$^{-/-}$ oocytes. The elevated phosphorylation of S6K1 at T389 had apparently led to an increase in its activity, as phosphorylation of S6K1 substrate, rpS6, was dramatically elevated in Oo*Tsc1*$^{-/-}$ oocytes (Fig. 5A, p-rpS6, S240/4 and S235/6).

In addition, the levels of phosphorylated eIF4B (Fig. 5A, p-eIF4B, S422) and total eIF4B (Fig. 5A), which is another S6K1 substrate that takes part in enhancing translation initiation (26), were higher in Oo*Tsc1*$^{-/-}$ oocytes than in Oo*Tsc1*$^{+/+}$ oocytes. These data indicate that mTORC1 activity is elevated in Oo*Tsc1*$^{-/-}$ oocytes.

Enhanced cap-dependent translation initiation in Oo*Tsc1*$^{-/-}$ oocytes

rpS6 is a substrate of S6K1 and is one of the 33 40S ribosomal proteins. 40S ribosomal subunits containing phosphorylated rpS6 are preferentially used during the formation of translation initiation complex (27). To determine the functional consequences of enhanced phosphorylation of rpS6 in Oo*Tsc1*$^{-/-}$ oocytes (Fig. 5A), we performed a cap-binding assay where the ability of rpS6 to bind the 7-methylguanosine cap structure (m7GTP) at the 5′-end of mRNAs was tested. Such binding occurs during cap-dependent initiation of translation (28).

We found that the ability of rpS6 to bind to m7GTP cap beads was significantly elevated in Oo*Tsc1*$^{-/-}$ oocytes when compared with that in Oo*Tsc1*$^{+/+}$ oocytes (Fig. 5B, rpS6 in m7GTP pull down). As a control, eIF4E, a cap-binding subunit of the translation initiation complex (28), showed similar affinity for cap beads in both Oo*Tsc1*$^{-/-}$ and Oo*Tsc1*$^{+/+}$ oocytes (Fig. 5B, eIF4E). This result suggests that elevated phosphorylation of rpS6 and eIF4B leads to enhanced cap-dependent translation initiation in Oo*Tsc1*$^{-/-}$ oocytes.

Activation of PI3K–Akt signaling is unaltered in Oo*Tsc1*$^{-/-}$ oocytes

We found that the level of p-Akt was not elevated in Oo*Tsc1*$^{-/-}$ oocytes, either at the basal level or after
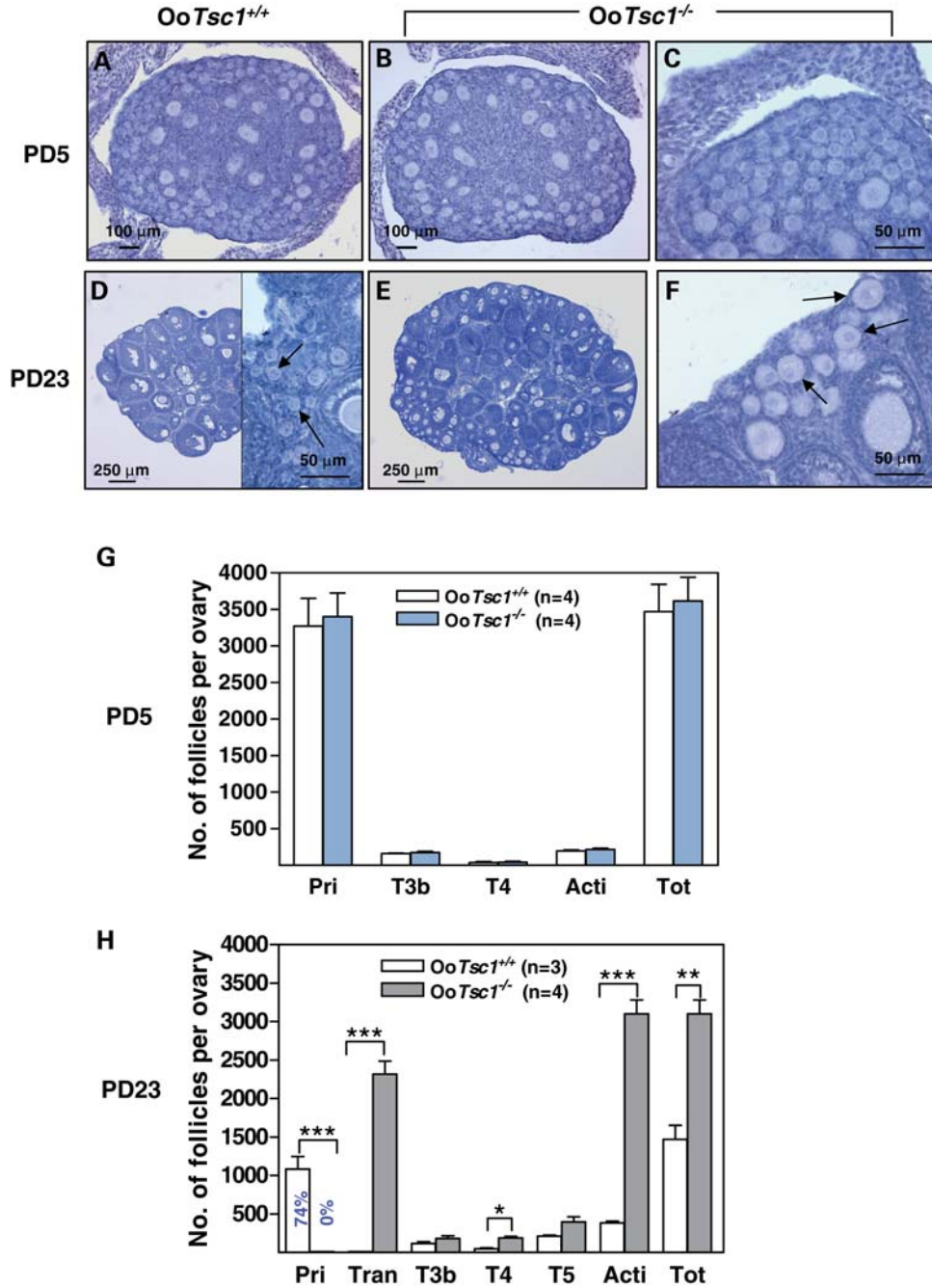
Figure 3. Activation of the entire pool of primordial follicles upon deletion of *Tsc1* from oocytes. (**A**–**F**) Morphological analysis of ovaries from Oo*Tsc1*⁻/⁻ and Oo*Tsc1*⁺/⁺ littermates at PD5 and PD23. Ovaries from 5- and 23-day-old Oo*Tsc1*⁺/⁺ and Oo*Tsc1*⁻/⁻ mice were embedded in paraffin, and serial sections of 8 μm thickness were prepared and stained with hematoxylin. At PD5, similar ovarian morphologies were seen in sections from Oo*Tsc1*⁺/⁺ and Oo*Tsc1*⁻/⁻ ovaries (A–C). At PD23, however, Oo*Tsc1*⁻/⁻ ovaries were larger (E) than Oo*Tsc1*⁺/⁺ ovaries (D). No primordial follicles could be seen by PD23 in Oo*Tsc1*⁻/⁻ ovaries, and almost all the primordial follicles were activated with apparently enlarged oocytes surrounded by flattened pregranulosa cells (F, arrows). In Oo*Tsc1*⁺/⁺ ovaries primordial follicles could be readily observed at PD23 (D, arrows). The experiments were repeated at least four times, and for each time and each age, ovaries from one mouse of each genotype were used. (**G** and **H**) Quantification of follicle numbers in ovaries of Oo*Tsc1*⁻/⁻ and Oo*Tsc1*⁺/⁺ littermates at PD5 and PD23. The numbers of different types of follicles per ovary (mean ± SEM) were quantified as described in Materials and Methods. Note that although similar numbers of follicles were seen in both genotypes at PD5 (G), no primordial follicles were observed in Oo*Tsc1*⁻/⁻ ovaries at PD23, whereas 74% of follicles were still at the primordial follicle stage in Oo*Tsc1*⁺/⁺ ovaries (H). Moreover, the numbers of activated follicles and of all follicles per Oo*Tsc1*⁻/⁻ ovary were significantly higher than for Oo*Tsc1*⁺/⁺ ovaries at PD23 (H). The numbers of mice used (*n*) and results of statistical analyses are given. $^*P < 0.05$, $^{**}P < 0.01$ and $^{***}P < 0.001$.
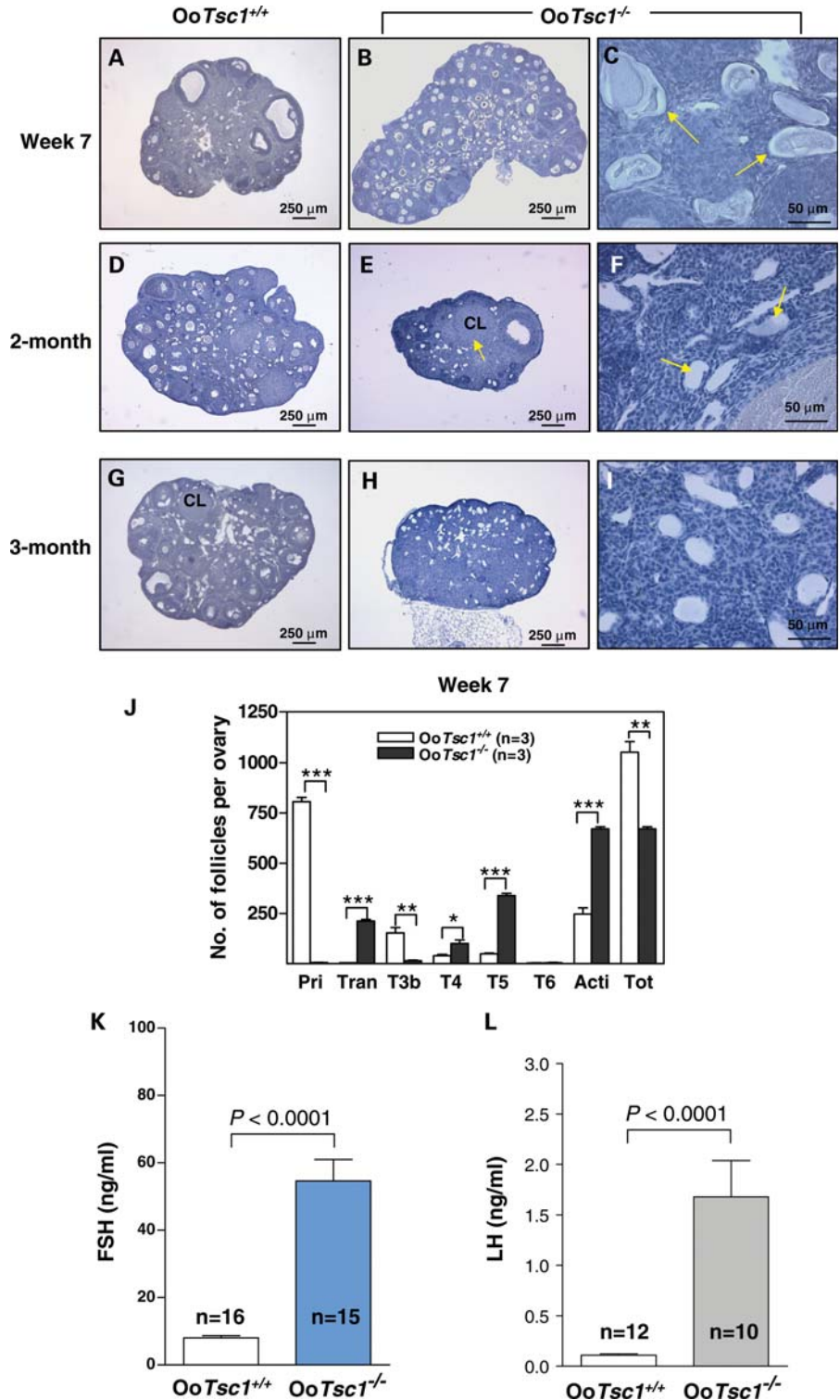
Figure 4. Follicle depletion and POF at young adulthood in Oo*Tsc1*$^{-/-}$ mice. (**A**–**I**) Morphological analysis of ovaries from Oo*Tsc1*$^{-/-}$ and Oo*Tsc1*$^{+/+}$ littermates at 7 weeks, 2 months and 3 months of age. Ovaries from Oo*Tsc1*$^{-/-}$ and Oo*Tsc1*$^{+/+}$ mice were embedded in paraffin and sections of 8 μm thickness were prepared and stained with hematoxylin. When compared with ovaries of Oo*Tsc1*$^{+/+}$ mice (A), Oo*Tsc1*$^{-/-}$ ovaries still appeared larger at 7 weeks of age (B). However, many activated follicles in Oo*Tsc1*$^{-/-}$ ovaries had already degenerated (C, arrows). At 2 months of age, almost all follicles had degenerated in Oo*Tsc1*$^{-/-}$ ovaries (F, arrows) and the ovaries were smaller (E) than Oo*Tsc1*$^{+/+}$ ovaries (D). By 3 months of age, healthy follicular structures had completely disappeared in Oo*Tsc1*$^{-/-}$ ovaries (H and I). Control Oo*Tsc1*$^{+/+}$ mice had normal ovarian morphology (G). CL, corpus luteum. (**J**) Quantification of follicle numbers in ovaries of 7-week-old Oo*Tsc1*$^{-/-}$ and Oo*Tsc1*$^{+/+}$ ovaries. The numbers of different types of follicles per ovary (mean $\pm$ SEM) were quantified as described in Materials and Methods. In 7-week-old Oo*Tsc1*$^{-/-}$ ovaries, the numbers of healthy follicles were significantly reduced compared with Oo*Tsc1*$^{+/+}$ ovaries. The numbers of mice used (*n*) and results of statistical analyses are given. **$P < 0.01$, ***$P < 0.001$. (**K** and **L**) Levels of FSH and LH in sera of 3- to 4-month-old Oo*Tsc1*$^{+/+}$ and Oo*Tsc1*$^{-/-}$ mice. FSH and LH were measured as described in Materials and Methods. Significantly elevated levels of FSH (K) and LH (L) in adult Oo*Tsc1*$^{-/-}$ mice were observed. The numbers of mice used (*n*) and *P*-values are shown in the figures.
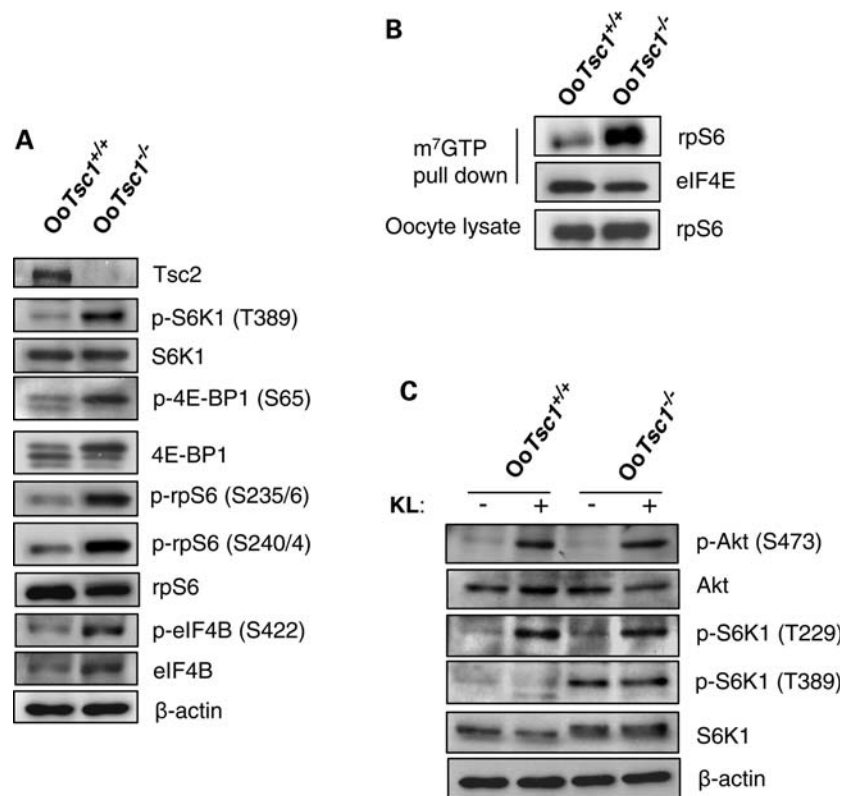
Figure 5. Studies of mTORC1 and PI3K signaling in OoTsc1$^{-/-}$ and OoTsc1$^{+/+}$ oocytes. (**A**) Comparison of Tsc1/mTORC1 signaling in OoTsc1$^{-/-}$ and OoTsc1$^{+/+}$ oocytes. Oocytes were isolated from ovaries of mice at PD12−14 and western blot was performed as described in Materials and Methods. Loss of *Tsc1* led to complete absence of Tsc2 protein in OoTsc1$^{-/-}$ oocytes. mTORC1 signaling in OoTsc1$^{-/-}$ oocytes was enhanced, as indicated by elevated levels of phosphorylated S6K1 (p-S6K1, T389) and phosphorylated rpS6 (p-rpS6, S235/6 and S240/4). Increased phosphorylation of 4E-BP1 (p-4E-BP1, S65) and eIF4B (p-eIF4B, S422), and elevated total protein levels of eIF4B were seen in OoTsc1$^{-/-}$ oocytes. Levels of total S6K1, rpS6, 4E-BP1 and β-actin were used as internal controls. (**B**) Enhanced cap-dependent translation initiation in OoTsc1$^{-/-}$ oocytes. Oocytes were isolated from ovaries of OoTsc1$^{-/-}$ and OoTsc1$^{+/+}$ mice at PD12−14 and cap-binding assays were performed as described in Materials and Methods. The ability of rpS6 to bind to m7GTP cap beads was found to be elevated in OoTsc1$^{-/-}$ oocytes compared with that in OoTsc1$^{+/+}$ oocytes. Equivalent amounts of protein between precipitates were monitored by the levels of eIF4E, which also binds to the m7GTP beads. Equal amounts of rpS6 in oocyte lysates were also shown. The experiments were repeated three times. For each experiment, material from 15−20 mice was used per lane. Representative images are shown. (**C**) Constitutively activated mTORC1 signaling, but unaltered PI3K−Akt signaling in OoTsc1$^{-/-}$ oocytes. Phosphorylation of S6K1 (p-S6K1, T389) was constitutively higher in OoTsc1$^{-/-}$ oocytes, which could not be elevated further by KL treatment. However, phosphorylation of Akt (p-Akt, S473) and S6K1 (p-S6K1, T229), which are activated by PI3K signaling, was similar in OoTsc1$^{-/-}$ and OoTsc1$^{+/+}$ oocytes both at the basal level and upon stimulation by KL (100 ng/ml, 2 min). Levels of total S6K1, Akt, rpS6 and β-actin were used as internal controls.

stimulation with Kit ligand (KL) (Fig. 5C, p-Akt, S473). Being a substrate of Akt, the phosphorylation of Foxo3a was not altered in OoTsc1$^{-/-}$ oocytes (data not shown), indicating that the activation status of Foxo3a was not altered. Moreover, phosphorylation of S6K1 at T229, which is performed by PDK1 (29), was unchanged in OoTsc1$^{-/-}$ oocytes—either at basal levels or upon stimulation with KL (Fig. 5C), indicating that the activation of PDK1 is not affected by loss of *Tsc1* in oocytes. These data support the idea that the activation of PI3K−PDK1−Akt signaling is unaltered in OoTsc1$^{-/-}$ oocytes, indicating that mTORC2 activity, which is responsible for phosphorylation of Akt at S473 (11), is not changed by the loss of *Tsc1*. As a comparison, the level of p-S6K1 at T389 (mediated by mTORC1) was constantly elevated in OoTsc1$^{-/-}$ oocytes and could not be stimulated further by treatment with KL (Fig. 5C).

For S6K1 to be active, its T389 and its T229 must both be phosphorylated (by mTORC1 and PDK1, respectively) (29). We found that the phosphorylation of S6K1 (T389) and

rpS6 (S235/6) in OoTsc1$^{-/-}$ oocytes were dependent on PI3K/Akt signaling, as pretreatment of OoTsc1$^{-/-}$ oocytes with a PI3K-specific inhibitor, LY294002, largely suppressed the phosphorylation of S6K1 (T389) and rpS6 (S235/6) (Fig. 6A, LY). This indicates that the activity of mTORC1 in oocytes is dependent on PI3K, although PI3K signaling *per se* is not changed due to loss of *Tsc1* (Fig. 5C).

Rapamycin effectively reverses the overactivation of primordial follicles in OoTsc1$^{-/-}$ ovaries

The phosphorylation of S6K1 (T389) and rpS6 (S235/6) in OoTsc1$^{-/-}$ oocytes was sensitive to the mTORC1-specific inhibitor rapamycin (Fig. 6A). To provide *in vivo* evidence that it is the elevated mTORC1 activity that drives the overactivation of primordial follicles in OoTsc1$^{-/-}$ mice, we injected rapamycin into OoTsc1$^{-/-}$ mice (5 mg/kg body weight per day), starting from PD4 for 19 days. The mice were sacrificed at PD23 and ovarian morphology was studied.
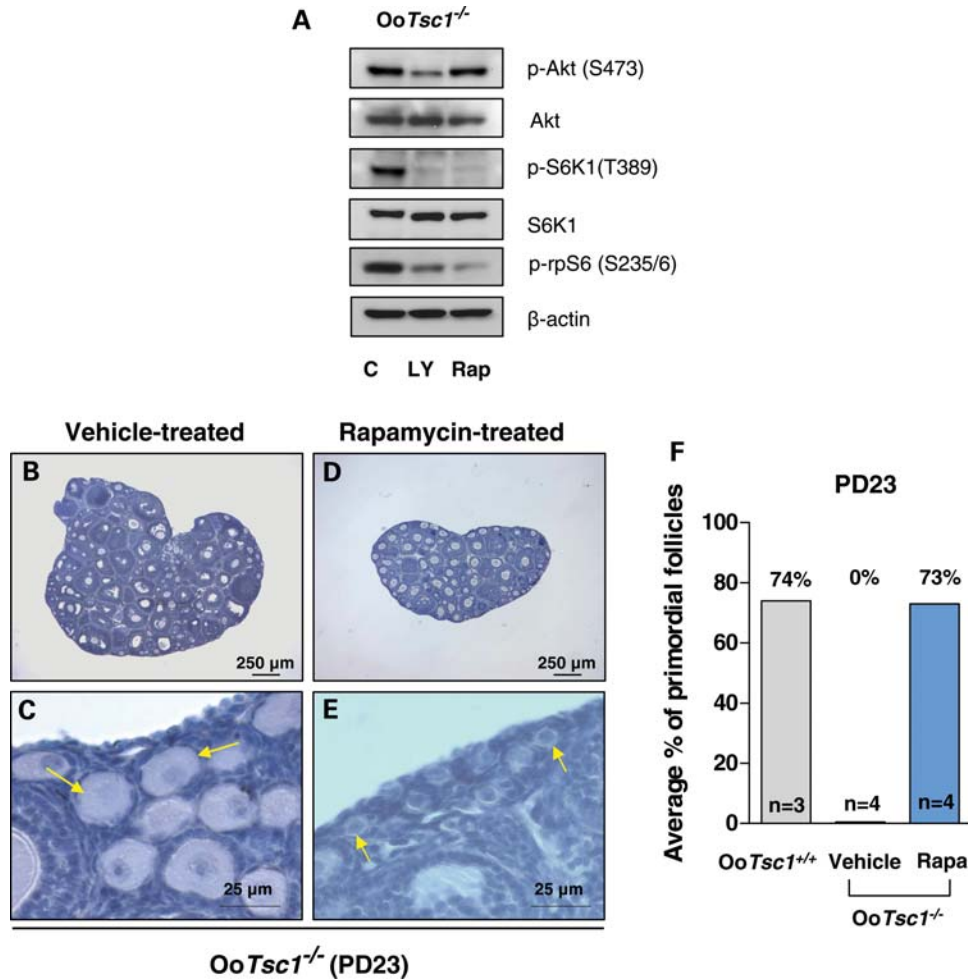
Figure 6. Rapamycin effectively reverses the overactivation of primordial follicles in Oo*Tsc1*$^{-/-}$ ovaries. (**A**) Activation of S6K1−rpS6 in Oo*Tsc1*$^{-/-}$ oocytes is dependent on PI3K and mTORC1 signaling. Oocytes were isolated from ovaries of Oo*Tsc1*$^{-/-}$ mice at PD12−14 as described in Materials and Methods. Treatment of oocytes with the PI3K-specific inhibitor LY294002 (LY, 50 μM) for 1 h was found to largely suppress levels of p-Akt (S473), p-S6K1 (T389) and p-rpS6 (S235/6), whereas treatment with the mTORC1-specific inhibitor rapamycin (Rap, 50 nM) for 1 h only suppressed the levels of p-S6K1 (T389) and p-rpS6 (S235/6), but not the level of p-Akt (S473) in Oo*Tsc1*$^{-/-}$ oocytes. This suggests that activation of S6K1−rpS6 in Oo*Tsc1*$^{-/-}$ oocytes is dependent on both PI3K and mTORC1 signaling. Levels of total Akt, S6K1 and β-actin were used as internal controls. (**B**−**E**) The overactivation of primordial follicles in Oo*Tsc1*$^{-/-}$ mice can be reversed by treatment with rapamycin. Rapamycin (5 mg/kg body weight) was injected daily into Oo*Tsc1*$^{-/-}$ mice from PD4 to PD22, and the ovaries were collected at PD23 for morphological analysis. Ovaries from rapamycin-treated Oo*Tsc1*$^{-/-}$ mice appeared smaller (D) than the ovaries from vehicle-treated Oo*Tsc1*$^{-/-}$ mice (B). Clusters of primordial follicles were seen in rapamycin-treated Oo*Tsc1*$^{-/-}$ mice at PD23 (E, arrows), whereas all primordial follicles were activated in vehicle-treated Oo*Tsc1*$^{-/-}$ mice at PD23 (C, arrows). (**F**) Proportions of primordial follicles (relative to the total number of follicles) in Oo*Tsc1*$^{+/+}$, Oo*Tsc1*$^{-/-}$ (vehicle-treated) and Oo*Tsc1*$^{-/-}$ (rapamycin-treated) ovaries at PD23. The average percentages of primordial follicles are shown. The proportion of primordial follicles in rapamycin-treated Oo*Tsc1*$^{-/-}$ ovaries was found to be elevated to 73%, which was similar to the proportion in Oo*Tsc1*$^{+/+}$ ovaries (74%). The numbers of mice used (*n*) are shown. Rapa, rapamycin.

We found that in PD23 Oo*Tsc1*$^{-/-}$ mice that had been treated with rapamycin, the ovaries were smaller (Fig. 6D) and typical primordial follicles were found (Fig. 6E, arrows). On the contrary, in ovaries of PD23 Oo*Tsc1*$^{-/-}$ mice that were treated with vehicle, the ovaries were larger (Fig. 6B) and all primordial follicles had been activated, with enlarged oocytes (Fig. 6C, arrows). Quantification of follicle numbers showed that the proportion of primordial follicles in rapamycin-treated Oo*Tsc1*$^{-/-}$ ovaries was elevated to 73%, which was similar to the proportion in Oo*Tsc1*$^{+/+}$ ovaries (74%) (Fig. 6F). These results clearly showed that elevated mTORC1 activity in oocytes is the major driving force that activates the whole pool of primordial follicles in

Oo*Tsc1*$^{-/-}$ mice. At the same time, this result also indicates that suppression of mTORC1 activity in oocytes is necessary for preservation of primordial follicles in a dormant state.

Tsc1 and PTEN in oocytes suppress follicular activation synergistically, but in distinct ways

We have reported earlier that mice lacking *Pten* in oocytes (referred to as Oo*Pten*$^{-/-}$ mice in this study) exhibit accelerated activation of primordial follicles (Fig. 7A) (8), which is most likely achieved through elevated phosphorylation of S6K1 at T229 (but not at T389), subsequently leading to
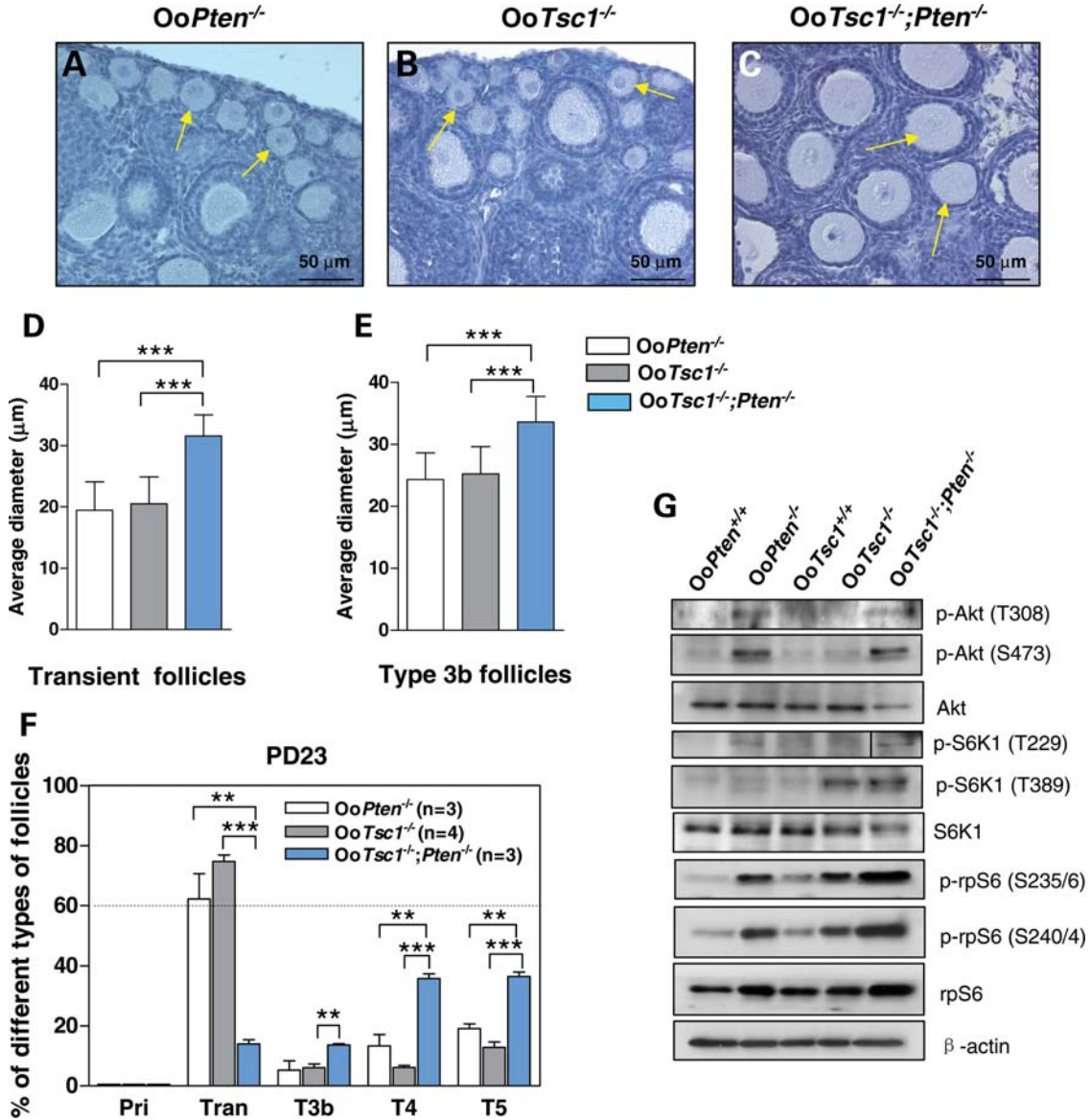
Figure 7. Tsc1 and PTEN in oocytes synergistically maintain the quiescence of primordial follicles through distinct ways. (**A**–**C**) Morphological analysis of ovaries from Oo*Pten*$^{-/-}$, Oo*Tsc1*$^{-/-}$ and Oo*Tsc1*$^{-/-}$;*Pten*$^{-/-}$ mice. At PD23, in Oo*Pten*$^{-/-}$ (A, arrows) and Oo*Tsc1*$^{-/-}$ ovaries (B, arrows) all primordial follicles were activated, with enlarged oocytes. It is noteworthy that in Oo*Tsc1*$^{-/-}$;*Pten*$^{-/-}$ ovaries, the rate of oocyte growth was further enhanced in a synergistic way (C, arrows) compared with that in singly mutated mice. (**D** and **E**) Average oocyte diameters in transient and type 3b follicles of PD23 Oo*Pten*$^{-/-}$, Oo*Tsc1*$^{-/-}$ and Oo*Tsc1*$^{-/-}$;*Pten*$^{-/-}$ ovaries. One hundred oocytes from randomly selected transient and type 3b follicles were measured as described in Materials and Methods. Oocytes in Oo*Tsc1*$^{-/-}$;*Pten*$^{-/-}$ follicles were found to be larger than those in Oo*Pten*$^{-/-}$ and Oo*Tsc1*$^{-/-}$ follicles. Results of statistical analyses are shown. ***$P < 0.001$. (**F**) Percentages of follicles at different developmental stages in Oo*Pten*$^{-/-}$, Oo*Tsc1*$^{-/-}$ and Oo*Tsc1*$^{-/-}$;*Pten*$^{-/-}$ ovaries at PD23. More than 60% of the activated follicles were at the transient follicle stage (Tran) in Oo*Pten*$^{-/-}$ and Oo*Tsc1*$^{-/-}$ ovaries, whereas in Oo*Tsc1*$^{-/-}$;*Pten*$^{-/-}$ ovaries more follicles were at further developed stages (including type 3b, type 4 and type 5 follicles). The numbers of mice used (*n*) and results of statistical analyses are given. **$P < 0.01$, *** $P < 0.001$. (**G**) Studies of PI3K and mTORC1 signaling in Oo*Pten*$^{+/+}$, Oo*Pten*$^{-/-}$, Oo*Tsc1*$^{+/+}$, Oo*Tsc1*$^{-/-}$ and Oo*Tsc1*$^{-/-}$;*Pten*$^{-/-}$ oocytes. In Oo*Pten*$^{-/-}$ oocytes, the levels of p-Akt (T308 and S473) and p-S6K1 (T229), but not of p-S6K1 (T389) were elevated. In comparison, in Oo*Tsc1*$^{-/-}$ oocytes, the levels of p-S6K1 (T389) but not of p-Akt (T308 and S473) or p-S6K1 (T229) were elevated. Nevertheless, in Oo*Tsc1*$^{-/-}$;*Pten*$^{-/-}$ oocytes, the levels of both p-Akt (T308 and S473) and p-S6K1 (T229 and T389) were elevated, indicating overactivation of both the PI3K and mTORC1 signaling in doubly mutated oocytes. As a consequence, the phosphorylation (indicating activation) of rpS6 (p-rpS6, S240/4 and S235/6) in Oo*Tsc1*$^{-/-}$;*Pten*$^{-/-}$ oocytes was further elevated compared with single-mutant Oo*Tsc1*$^{-/-}$ or Oo*Pten*$^{-/-}$ oocytes. Moreover, the protein levels of rpS6 were also higher in Oo*Tsc1*$^{-/-}$;*Pten*$^{-/-}$ oocytes. Levels of total Akt, S6K1 and β-actin were used as internal controls. All experiments were repeated three times. For each experiment, material from 3–5 mice was used per lane. In each lane, 20–30 µg of protein sample was loaded. Representative images are shown.

enhanced phosphorylation of rpS6 (S235/6 and S240/4) in Oo*Pten*$^{-/-}$ oocytes (9). In the current study, we found that loss of *Tsc1* in oocytes leads to enhanced phosphoryl-ation of S6K1 at T389 (Fig. 5A), but not at T229 (Fig. 5C). This also leads to elevated activation of rpS6 (Fig. 5A).

To determine the functional relationship between the PTEN/PI3K signaling and the Tsc/mTORC1 signaling within the oocyte in regulating follicular activation, we crossed Oo*Tsc1*$^{-/-}$ mice with Oo*Pten*$^{-/-}$ mice and studied follicular development in progeny mice with concurrent loss of *Tsc1* and *Pten* in oocytes (referred to as Oo*Tsc1*$^{-/-}$;*Pten*$^{-/-}$ mice). We found that in Oo*Tsc1*$^{-/-}$;*Pten*$^{-/-}$ mice, the rate of oocyte growth was synergistically enhanced further (as shown in the ovaries of PD23 mice; Fig. 7C, arrows) when compared with that in single mutant Oo*Pten*$^{-/-}$ ovaries (Fig. 7A, arrows) or Oo*Tsc1*$^{-/-}$ ovaries (Fig. 7B, arrows).

To further characterize the rate of oocyte growth in Oo*Tsc1*$^{-/-}$;*Pten*$^{-/-}$ mice, we measured the diameters of oocytes of transient and type 3b follicles in these mice. We found that the average diameters of oocytes in transient follicles (Fig. 7D) and type 3b follicles (Fig. 7E) in Oo*Tsc1*$^{-/-}$;*Pten*$^{-/-}$ ovaries were significantly larger than those in Oo*Pten*$^{-/-}$ and Oo*Tsc1*$^{-/-}$ ovaries. In addition, in Oo*Pten*$^{-/-}$ and Oo*Tsc1*$^{-/-}$ ovaries, by PD23 more than 60% of activated follicles were at the transient follicle stage (Fig.7F, Tran), whereas in Oo*Tsc1*$^{-/-}$;*Pten*$^{-/-}$ ovaries significantly more follicles were found to be type 3b, type 4 and type 5 follicles (Fig. 7F, T3b, T4 and T5). These results suggest that the concurrent deficiencies of *Tsc1* and *Pten* in oocytes result in synergistically enhanced oocyte growth and follicular development in Oo*Tsc1*$^{-/-}$;*Pten*$^{-/-}$ ovaries.

To characterize the underlying signaling events that drive the enhanced rate of oocyte growth in Oo*Tsc1*$^{-/-}$;*Pten*$^{-/-}$ mice, we studied the activation status of PI3K signaling and mTORC1 signaling in doubly mutated oocytes in comparison to singly mutated Oo*Tsc1*$^{-/-}$ or Oo*Pten*$^{-/-}$ oocytes.

As shown in Figure 7G, in Oo*Pten*$^{-/-}$ oocytes the levels of p-Akt (T308 and S473) and p-S6K1 (T229), but not p-S6K1 (T389), were elevated. In comparison, in Oo*Tsc1*$^{-/-}$ oocytes the levels of p-S6K1 (T389) were elevated, whereas levels of p-Akt (T308 or S473) or p-S6K1 (T229) were not elevated (Fig. 7G).

In Oo*Tsc1*$^{-/-}$;*Pten*$^{-/-}$ oocytes, the phosphorylation of Akt at both T308 and S473 (Fig. 7G, p-Akt, T308 and S473) and the phosphorylation of S6K1 at T229 and T389 (Fig. 7G, p-S6K1, T229 and T389) were elevated, indicating a constitutive overactivation of both the pI3K signaling and the mTORC1 signaling in the doubly mutated oocytes. As a consequence, the phosphorylation (indicating activation) of rpS6 in Oo*Tsc1*$^{-/-}$;*Pten*$^{-/-}$ oocytes was further elevated compared with single-mutant Oo*Tsc1*$^{-/-}$ or Oo*Pten*$^{-/-}$ oocytes (Fig. 7G, p-rpS6, S235/6, S240/4). Moreover, the expression of rpS6 was also elevated in Oo*Tsc1*$^{-/-}$;*Pten*$^{-/-}$ oocytes (Fig. 7G, rpS6), which is probably a consequence of enhanced protein translation in the doubly mutated oocytes.

Thus, in combination with our earlier studies on the Oo*Pten*$^{-/-}$ mice (8,9), our results show that loss of *Tsc1* or *Pten* in oocytes both lead to overactivation of rpS6, but through distinct signaling pathways. PTEN in oocytes suppresses follicular activation through negative regulation of the PI3K signaling, which subsequently inhibits phosphorylation of S6K1 at its T229 (9) (Fig. 9, T229 of S6K1); whereas Tsc1 in oocytes suppresses follicular activation by negative regulation of mTORC1 signaling, which subsequently suppresses the phosphorylation of S6K1 at its T389 (Fig. 9, T389 of S6K1). Our results thus indicate that the function of either Tsc1 or PTEN is necessary, but not sufficient, to maintain the quiescence of primordial follicles. In order to prevent premature follicular activation, a synergistically combined function of Tsc1 and PTEN is needed to negatively regulate the activation of S6K1–rpS6 signaling in oocytes.

PDK1 signaling is required for functional S6K1–rpS6 in Oo*Tsc1*$^{-/-}$ oocytes

PDK1 is responsible for phosphorylating T229 of S6K1. To study the functional contribution of PDK1 signaling in the excessive follicular activation in Oo*Tsc1*$^{-/-}$ ovaries, we crossed Oo*Tsc1*$^{-/-}$ mice with Oo*Pdk1*$^{-/-}$ mice (9) and studied follicular development in the progeny (referred to as Oo*Tsc1*$^{-/-}$;*Pdk1*$^{-/-}$ mice). In Oo*Tsc1*$^{-/-}$ ovaries, all primordial follicles were activated by PD23 (Fig. 8B, arrows), and the proportion of primordial follicles (compared with the total number of follicles) was 0% (Fig. 8E). In Oo*Tsc1*$^{-/-}$;*Pdk1*$^{-/-}$ ovaries of the same age, however, clusters of primordial follicles were seen (Fig. 8D, arrows), the proportion of which was elevated to 52% (Fig. 8E). These results show that the loss of *Pdk1* in oocytes partly reversed the overactivation of primordial follicles in Oo*Tsc1*$^{-/-}$ ovaries.

In Oo*Tsc1*$^{-/-}$ oocytes, S6K1 and rpS6 were overactivated (Fig. 5A). This overactivation of S6K1 signaling was caused by elevated phosphorylation of its T389 by mTORC1 (Fig. 5A, p-S6K1, T389). On the other hand, activation of S6K1 also requires phosphorylation of its T229. We found that the levels of phosphorylated rpS6 and total rpS6 were largely reduced in Oo*Tsc1*$^{-/-}$;*Pdk1*$^{-/-}$ oocytes (Fig. 8F, p-rpS6, S240/4 and rpS6), which was likely caused by less activity of S6K1 due to downregulation of PDK1-mediated phosphorylation at its T229 (Fig. 8F, p-S6K1, T229). Thus, the downregulation of expression and phosphorylation of rpS6 in Oo*Tsc1*$^{-/-}$;*Pdk1*$^{-/-}$ oocytes may be the reason for prevention of the excessive follicular activation seen in Oo*Tsc1*$^{-/-}$ ovaries. Thus, it is likely that the activation of primordial follicles is dependent on both mTOR signaling and PDK1 function.

DISCUSSION

In this study, by using a mutant mouse model with oocyte-specific deletion of *Tsc1*, we found that the tumor suppressor Tsc1 functions in oocytes to suppress follicular activation. Upon deletion of *Tsc1* in oocytes, the entire pool of primordial follicles is prematurely activated. We also found that the driving force underlying the overactivation of primordial follicles in Oo*Tsc1*$^{-/-}$ ovaries is elevated mTORC1 activity, which enhances the activation of S6K1–rpS6 signaling that promotes protein translation and ribosomal biogenesis in oocytes. These findings are corroborated by our parallel report with mice lacking the *Tsc2* gene in oocytes (the Oo*Tsc2*$^{-/-}$ mice), in which an almost identical phenotype was observed (30). Therefore, our studies indicate that the tumor suppressors Tsc1 and Tsc2 play physiological roles in oocytes to suppress the activation of primordial follicles. On
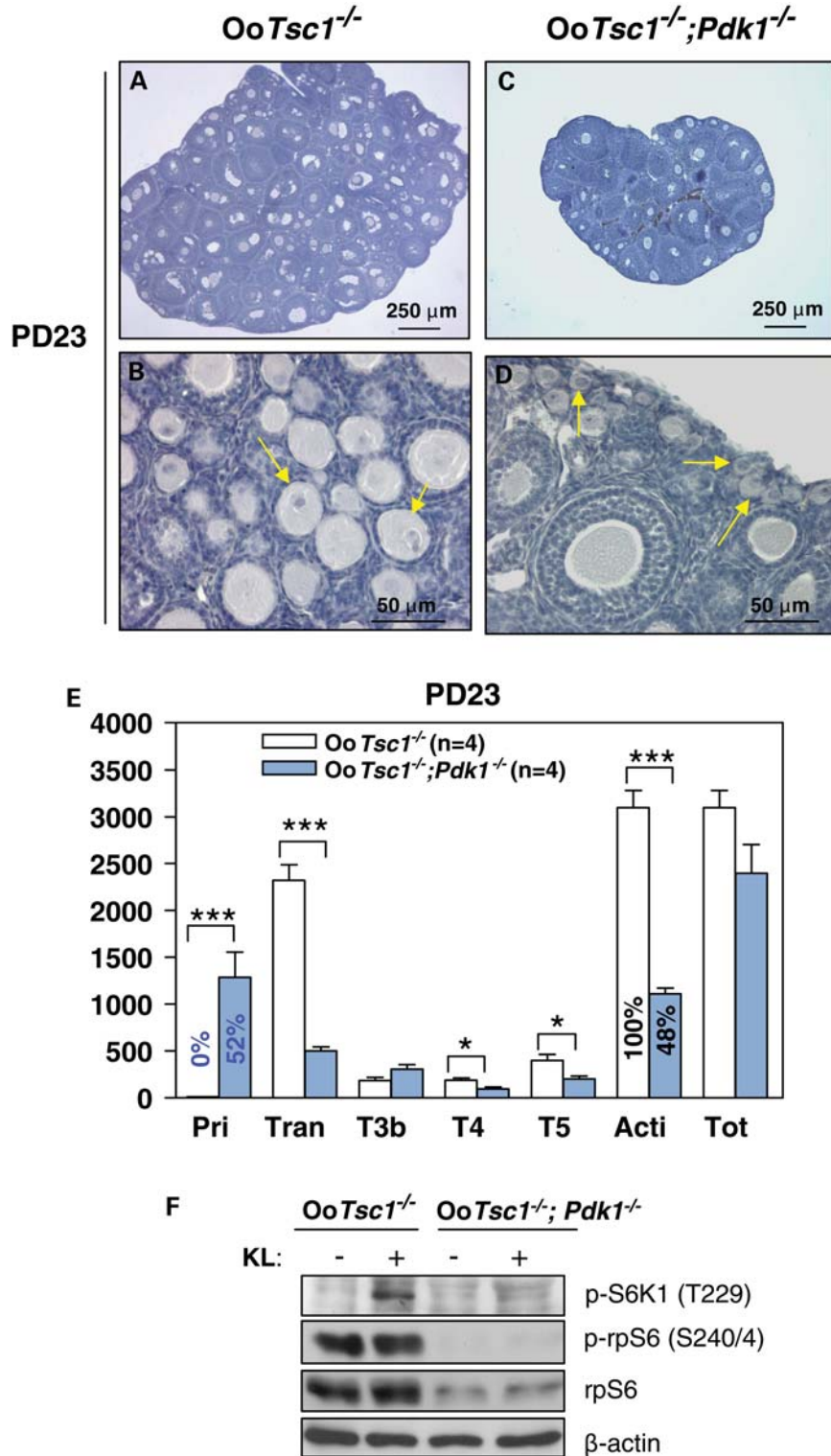
Figure 8. Concurrent loss of *Tsc1* and *Pdk1* in oocytes largely prevents the overactivation of primordial follicles in Oo*Tsc1*$^{-/-}$ ovaries. (**A**–**D**) Morphological analysis of ovaries from Oo*Tsc1*$^{-/-}$ and Oo*Tsc1*$^{-/-}$;*Pdk1*$^{-/-}$ mice at PD23. In Oo*Tsc1*$^{-/-}$ ovaries, all primordial follicles were activated (B, arrows). However, in Oo*Tsc1*$^{-/-}$;*Pdk1*$^{-/-}$ mice, clusters of primordial follicles were observed (D, arrows). As a result of there being less follicular activation, Oo*Tsc1*$^{-/-}$;*Pdk1*$^{-/-}$ ovaries were smaller (C) than Oo*Tsc1*$^{-/-}$ ovaries (A). (**E**) Quantification of follicle numbers in ovaries of Oo*Tsc1*$^{-/-}$ and Oo*Tsc1*$^{-/-}$;*Pdk1*$^{-/-}$ mice at PD23. The numbers of different types of follicles per ovary (mean ± SEM) were quantified as described in Materials and Methods. No typical primordial follicles were observed in Oo*Tsc1*$^{-/-}$ ovaries (0%) at PD23, whereas 52% of follicles in Oo*Tsc1*$^{-/-}$;*Pdk1*$^{-/-}$ ovaries were at the primordial stage. The numbers of mice used (*n*) and results of statistical analyses are given. *$P < 0.05$, ***$P < 0.001$. (**F**) Comparison of activation of S6K1–rpS6 signaling in Oo*Tsc1*$^{-/-}$ and Oo*Tsc1*$^{-/-}$;*Pdk1*$^{-/-}$ oocytes. Oocytes were isolated from ovaries of mice at PD12–14 and western blot was performed as described in Materials and Methods. KL treatment (100 ng/ml, 2 min) was found to lead to a rapid phosphorylation of S6K1 at T229 in Oo*Tsc1*$^{-/-}$ oocytes, but not in Oo*Tsc1*$^{-/-}$;*Pdk1*$^{-/-}$ oocytes, indicating that S6K1 can not be efficiently activated in Oo*Tsc1*$^{-/-}$;*Pdk1*$^{-/-}$ oocytes. The phosphorylation of rpS6 (p-rpS6, S240/4) and rpS6 expression were downregulated in Oo*Tsc1*$^{-/-}$;*Pdk1*$^{-/-}$ oocytes. The level of β-actin was used as internal control.
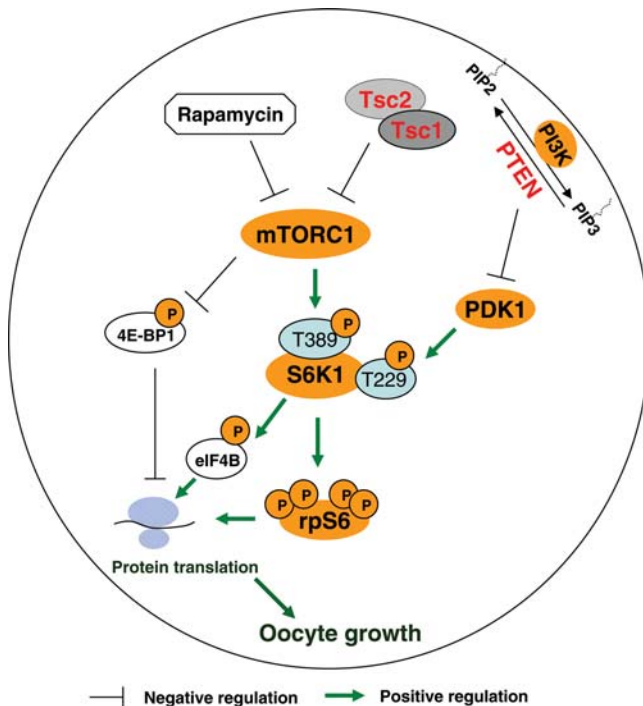
Figure 9. Tsc/mTORC1 and PTEN/PI3K signaling in oocytes controls the quiescence and activation of primordial follicles in a synergistic and collaborative way. On the basis of the evidence accumulated, we propose that PTEN in oocytes suppresses follicular activation through negative regulation of the PI3K signaling and of the function of PDK1, which leads to subsequent inhibition of phosphorylation of S6K1 at T229 by PDK1 (9). On the other hand, Tsc1 in oocytes suppresses follicular activation by negative regulation of mTORC1 signaling, leading to suppressed phosphorylation of S6K1 at T389. Thus, in this scheme both PTEN and Tsc suppress the phosphorylation/activation of rpS6, but by regulating the phosphorylation of distinct threonine residues in S6K1. We propose that collaborative, synergistic functions of Tsc1–Tsc2 and PTEN are required to negatively regulate the activation of S6K1–rpS6 signaling, which in turn facilitate maintenance of the quiescence of primordial follicles. A reduction in the activities of Tsc1–Tsc2 or PTEN, or both, would lead to premature follicular activation. Also shown in the illustration is rapamycin, which is an mTORC1 specific inhibitor. P, phosphorylation; PIP2, phosphatidylinositol-4,5-bisphosphate; PIP3, phosphatidylinositol 3,4,5-trisphosphate.

the basis of our results, we suggest that suppression of mTORC1 activity by the Tsc1–Tsc2 complex in oocytes is a prerequisite for maintenance of the quiescent state of primordial follicles in mice, which is required for preservation of the length of female reproductive life. At the same time, our results also indicate that elevated mTORC1 activity in the oocyte is required for follicular activation in mice. We conclude that Tsc/mTORC1 signaling in oocytes plays an indispensable role in preserving the primordial follicles in their dormant state and in triggering the activation of selected primordial follicles.

Our earlier reports have shown that the PTEN/PI3K–PDK1 signaling is of importance in controlling different developmental courses of primordial follicles (8,9). Deletion of *Pten* from mouse oocytes leads to premature activation of the entire pool of primordial follicles (8), and deletion of *Pdk1* in oocytes leads to accelerated depletion of primordial follicles (9). In the current work, we have shown that the Tsc/mTORC1 signaling in oocytes is equally important for preservation of

the primordial follicles in their dormant state, and it controls the activation of primordial follicles. Even so, although the overactivation of primordial follicles observed in Oo*Tsc1*$^{-/-}$ mice is phenotypically similar to that seen in Oo*Pten*$^{-/-}$ mice, the Tsc/mTORC1 signaling in oocytes regulates follicular dormancy and activation in a more distinct way than PTEN. Although both Tsc and PTEN manipulate follicular activation through negative regulation of the activation of S6K1–rpS6 in oocytes, Tsc suppresses the phosphorylation of S6K1 at its T389, as shown in the current study, whereas PTEN suppresses the phosphorylation of S6K1 at its T229, as shown earlier (9). Suppression of phosphorylation of both threonine sites results in inhibition of S6K1–rpS6 activation in oocytes, which helps to preserve the quiescence of primordial follicles. Thus, our results from the Oo*Tsc1*$^{-/-}$ and Oo*Pten*$^{-/-}$ mice show that elevated phosphorylation of either T389 or T229 of S6K1, due to deletion of *Tsc1* or *Pten*, leads to enhanced activation of S6K1–rpS6 signaling, which subsequently causes accelerated protein translation in oocytes. This appears to be the reason for the rapid oocyte enlargement and accelerated follicular activation seen in Oo*Tsc1*$^{-/-}$ and Oo*Pten*$^{-/-}$ mice.

Interestingly, although Tsc/mTORC1 signaling has been proposed to be downstream of PTEN/PI3K signaling in some cell types (15), the functions of both PTEN and Tsc1 in maintaining the quiescence of primordial follicles do not seem to be in a upstream and downstream arrangement in mouse oocytes. Instead, PTEN and Tsc1 appear to suppress follicular activation in parallel, in a synergistic and collaborative way. This notion is supported by our results that double deletion of *Tsc1* and *Pten* leads to further synergistically enhanced oocyte growth when compared with singly mutated mice. These results indicate that in order to maintain the quiescence of primordial follicles, phosphorylation of both T389 and T229 of S6K1 in oocytes must be suppressed by Tsc and PTEN, respectively (Fig. 9), through which the activation of S6K1–rpS6 signaling is suppressed. As a result, primordial follicles are prevented from being activated. At the same time, activation of primordial follicles seems to depend on the functioning of both intra-oocyte mTOR and PDK1 signaling, a notion that is supported by our finding that overactivation of primordial follicles in Oo*Tsc1*$^{-/-}$ ovaries was largely reversed by concurrent loss of *Pdk1*.

The regulation of Tsc/mTORC1–S6K1–rpS6 signaling in oocytes is likely to play a role in determining the course of development of primordial follicles. It is possible that Tsc adjusts mTORC1 activity in oocytes to an optimal level, so that the pool of primordial follicles is maintained in a dormant but surviving condition. On the other hand, demise of primordial follicles could be caused by suppression of mTORC1 signaling in oocytes, and activation of primordial follicles appears to be the result of elevated mTORC1 activity in oocytes. On the basis of the several lines of evidence accumulated, we believe that the Tsc/mTORC1–S6K1–rpS6 signaling and the PTEN/PI3K–PDK1–S6K1–rpS6 signaling in oocytes regulate the development of primordial follicles in a coordinated way, which ensures the proper length of female reproductive life.

More than a decade ago, it was hypothesized that resting primordial follicles may be under constant inhibitory

influences of local origin to remain dormant (31). In recent years, this hypothesis has been shown to be true with several lines of evidence from genetically modified mouse models (reviewed in 3,32). It is apparent now that Tsc1, Tsc2 and PTEN in oocytes are part of the inhibitory mechanisms that maintain the quiescence of primordial follicles. Other similar inhibitory molecules include the cyclin-dependent kinase (Cdk) inhibitor p27[kip1] (p27 or Cdkn1b) (33), which functions in both oocytes and pregranulosa cells to suppress follicular activation, and Foxo3a, a transcription factor that functions downstream of PTEN/PI3K signaling (8) in oocytes and suppresses follicular activation (34,35).

It is noteworthy that mice lacking *Tsc1*, *Tsc2* and *Pten* in oocytes, or mice lacking *p27*, all suffer from POF (8,30,33). The POF in these mutant mice is caused by a similar overactivation of the follicular pool, which is followed by follicular depletion. On the contrary, deletion of *Pdk1* or *Rps6* in oocytes also causes POF, but as a result of accelerated depletion of primordial follicles directly from their dormant state (9). Thus, the two types of POF, as observed in different mutant mouse models, may represent distinct etiologies of POF in humans.

In women, reproductive lifespan and menopausal age are determined by the ovarian reserve, i.e. by the size and persistence of the primordial follicle pool. The results of the current study and recent reports suggest that the deregulation of signaling events in oocytes such as Tsc/mTORC1 signaling, PTEN/PI3K signaling (8,9) and the p27-Cdk system (33), may also be the reasons for the defects in primordial follicle development in humans, which can result in pathological conditions of the ovary, including POF and infertility. In this sense, our work may have broad physiological and clinical implications. We believe that comprehension of signaling networks in oocytes will open up new avenues for a better understanding of ovarian physiology and pathology.

MATERIALS AND METHODS

Mice

$Tsc1^{loxP/loxP}$ mice with a mixed genomic background of 129S4/SvJae and C57BL/6J (14), $Pten^{loxP/loxP}$ mice (8) and $Pdk1^{loxP/loxP}$ mice (36,37) with a C57BL/6J genomic background were crossed with transgenic mice that carried *Gdf-9* promoter-mediated Cre recombinase which had a C57BL/6J background (8,18). After multiple rounds of crossing, we obtained homozygous mutant female mice lacking *Tsc1* in oocytes (Oo$Tsc1^{-/-}$ mice), mice lacking *Pten* in oocytes (Oo$Pten^{-/-}$ mice), mice lacking both *Tsc1* and *Pten* in oocytes (Oo$Tsc1^{-/-}$;$Pten^{-/-}$ mice) and mice lacking both *Tsc1* and *Pdk1* in oocytes (Oo$Tsc1^{-/-}$;$Pdk1^{-/-}$ mice). Control mice that do not carry the Cre transgene are referred to as Oo$Tsc1^{+/+}$, Oo$Pten^{+/+}$ or Oo$Pdk1^{+/+}$ mice. The mice were housed under controlled environmental conditions with free access to water and food. Illumination was on between 06.00 and 18.00 h. Experimental protocols were approved by the regional Ethics Committee of Umeå University, Sweden.

Reagents, antibodies and immunological detection methods

The rabbit polyclonal antibodies to Akt, phospho-Akt (S473), phospho-rpS6 (S235/236 and S240/244), tuberin/Tsc2, hamartin/Tsc1, phospho-eIF4B (S422), eIF4B, phospho-4E-BP1 (S65) and phospho-S6K1 (T389) and also rabbit monoclonal antibodies to eIF4E, 4E-BP1 and S6K1 were obtained from Cell Signaling Technologies (Beverly, MA, USA). Mouse monoclonal antibody to rpS6 was purchased from Santa Cruz Biotechnology Inc. (Santa Cruz, CA, USA). The polyclonal antibody to phospho-S6K1 (T229) was purchased from R&D Systems (Minneapolis, MN, USA). Mouse monoclonal antibody to β-actin, polyethylene glycol 400 and Tween-80 were purchased from Sigma-Aldrich Sweden AB (Stockholm, Sweden). 7-Methyl GTP-sepharose was purchased from GE Healthcare (Buckinghamshire, UK). The PI3K-specific inhibitor LY 294002, the mTORC1-specific inhibitor rapamycin and recombinant mouse KL were obtained from EMD Biosciences (San Diego, CA, USA). Western blots were carried out according to the instructions of the suppliers of the different antibodies and visualized using the ECL Plus Western Blotting Detection System (Amersham Biosciences, Uppsala, Sweden).

Quantification of ovarian follicles and histological analysis

Quantification of ovarian follicles was performed as previously described (8). Briefly, ovaries were fixed in 4% paraformaldehyde, dehydrated and embedded in paraffin. To count the numbers of follicles, paraffin-embedded ovaries were serially sectioned at 8 μm thickness and stained with hematoxylin for morphological observation. Ovarian follicles at different stages of development, including primordial follicles and activated follicles (including transient follicles containing enlarged oocytes surrounded by flattened pregranulosa cells, type 3b, type 4, type 5 and type 6 follicles) were counted in all sections of an ovary, based on the well-accepted standards established by Pedersen and Peters (38). Follicles that contained oocytes with clearly visible nuclei were scored in each section, as previously reported (39). Judged from careful morphological analysis, the incidence of counting the same follicle twice or of missing a follicle was low.

Measurement of oocyte diameters in transient and primary follicles

One hundred transient follicles and 100 primary (type 3b) follicles were randomly selected from paraffin sections of ovaries from at least three mice of each genotypes. The diameters of oocytes were measured using AxioVision software release 4.2 (Carl Zeiss MicroImaging GmbH, Göttingen, Germany) and a Leica DMLB microscope.

Isolation of oocytes from post-natal mouse ovaries and stimulation of starved oocytes with KL

Isolation and lysis of oocytes were performed as previously described (8). For stimulation with KL, equal amounts of oocytes were aliquoted into wells of a 24-well plate. Typically, each well contained oocytes obtained from 3–5 Oo$Tsc1^{-/-}$ and Oo$Tsc1^{+/+}$ mice that were 12–14 days old.

The oocytes were first starved by culturing them in serum-free DMEM/F12 medium for 4 h, followed by treatment with 100 ng/ml KL for 2 min. After stimulation with KL, the 24-well plate was chilled on ice and oocytes were lysed for western blot analysis.

Cap-binding assay

The 5′-end of all nuclear-transcribed mRNAs carries a 7-methylguanosine cap structure (m^7GpppN, where N represents any nucleotide) (40). Phosphorylation of rpS6 facilitates its recruitment to the cap complex and stimulates assembly of the translation initiation complex (41). To measure the ability of rpS6 in oocytes to bind to the 7-methylguanosine cap complex, $50–100\,\mu g$ of oocyte lysate was incubated with 7-methyl-GTP Sepharose beads for 2 h. Immunoprecipitates were washed three times in lysis buffer and were subjected to western blot for detection of rpS6. Equivalent levels of protein between precipitates were monitored through analysis of eIF4E, a cap-binding subunit of the translation initiation complex (40).

Measurement of serum hormone levels

Adult female Oo*Tsc1*$^{-/-}$ mice of 3- to 4-month-old were killed randomly due to lack of regular estrus cycles; control Oo*Tsc1*$^{+/+}$ female mice of similar age were killed at the estrus stage based on vaginal smears, in order to measure gonadotropin levels during the follicular growth phase but not the ovulation phase. Serum hormone levels were determined by immunoassay as described previously for FSH (42) and LH (43).

In vivo treatment of Oo*Tsc1*$^{-/-}$ mice with rapamycin

Rapamycin was dissolved in a vehicle containing 5.2% Tween-80 and 5.2% polyethylene glycol 400. For daily intraperitoneal injection of the mice, a dosage of 5 mg/kg body weight was used. The Oo*Tsc1*$^{-/-}$ and Oo*Tsc1*$^{+/+}$ mice were injected daily from PD4 to PD22 and were killed at PD23. The ovaries were then fixed in 4% paraformaldehyde, dehydrated and embedded in paraffin. For morphological observation, paraffin-embedded ovaries were sectioned at $8\,\mu m$ thickness and stained with hematoxylin. As controls, mice injected with vehicle were used.

Statistical analysis

All experiments were repeated at least three times. For comparisons of follicle numbers and hormone levels, differences between the two groups were calculated with Student's *t*-test, and a difference was considered to be significant if $P < 0.05$.

ACKNOWLEDGEMENTS

Conflict of Interest statement. None declared.

FUNDING

REFERENCES

1. Hirshfield, A.N. (1991) Development of follicles in the mammalian ovary. *Int. Rev. Cytol.*, **124**, 43–101.
2. McGee, E.A. and Hsueh, A.J. (2000) Initial and cyclic recruitment of ovarian follicles. *Endocr. Rev.*, **21**, 200–214.
3. Adhikari, D. and Liu, K. (2009) Molecular mechanisms underlying the activation of mammalian primordial follicles. *Endocr. Rev.*, **30**, 438–464.
4. Broekmans, F.J., Knauff, E.A., te Velde, E.R., Macklon, N.S. and Fauser, B.C. (2007) Female reproductive ageing: current knowledge and future trends. *Trends Endocrinol. Metab.*, **18**, 58–65.
5. Faddy, M.J., Gosden, R.G., Gougeon, A., Richardson, S.J. and Nelson, J.F. (1992) Accelerated disappearance of ovarian follicles in mid-life: implications for forecasting menopause. *Hum. Reprod.*, **7**, 1342–1346.
6. Hansen, K.R., Knowlton, N.S., Thyer, A.C., Charleston, J.S., Soules, M.R. and Klein, N.A. (2008) A new model of reproductive aging: the decline in ovarian non-growing follicle number from birth to menopause. *Hum. Reprod.*, **23**, 699–708.
7. Liu, K., Rajareddy, S., Liu, L., Jagarlamudi, K., Boman, K., Selstam, G. and Reddy, P. (2006) Control of mammalian oocyte growth and early follicular development by the oocyte PI3 kinase pathway: new roles for an old timer. *Dev. Biol.*, **299**, 1–11.
8. Reddy, P., Liu, L., Adhikari, D., Jagarlamudi, K., Rajareddy, S., Shen, Y., Du, C., Tang, W., Hamalainen, T., Peng, S.L. *et al.* (2008) Oocyte-specific deletion of Pten causes premature activation of the primordial follicle pool. *Science*, **319**, 611–613.
9. Reddy, P., Adhikari, D., Zheng, W., Liang, S., Hamalainen, T., Tohonen, V., Ogawa, W., Noda, T., Volarevic, S., Huhtaniemi, I. and Liu, K. (2009) PDK1 signaling in oocytes controls reproductive aging and lifespan by manipulating the survival of primordial follicles. *Hum. Mol. Genet.*, **18**, 2813–2824.
10. Guertin, D.A. and Sabatini, D.M. (2007) Defining the role of mTOR in cancer. *Cancer Cell*, **12**, 9–22.
11. Sarbassov, D.D., Guertin, D.A., Ali, S.M. and Sabatini, D.M. (2005) Phosphorylation and regulation of Akt/PKB by the rictor-mTOR complex. *Science*, **307**, 1098–1101.
12. Wullschleger, S., Loewith, R. and Hall, M.N. (2006) TOR signaling in growth and metabolism. *Cell*, **124**, 471–484.
13. Crino, P.B., Nathanson, K.L. and Henske, E.P. (2006) The tuberous sclerosis complex. *N. Engl. J. Med.*, **355**, 1345–1356.
14. Kwiatkowski, D.J., Zhang, H., Bandura, J.L., Heiberger, K.M., Glogauer, M., el Hashemite, N. and Onda, H. (2002) A mouse model of TSC1 reveals sex-dependent lethality from liver hemangiomas, and up-regulation of p70S6 kinase activity in Tsc1 null cells. *Hum. Mol. Genet.*, **11**, 525–534.
15. Yang, Q. and Guan, K.L. (2007) Expanding mTOR signaling. *Cell Res.*, **17**, 666–681.
16. Chong-Kopera, H., Inoki, K., Li, Y., Zhu, T., Garcia-Gonzalo, F.R., Rosa, J.L. and Guan, K.L. (2006) TSC1 stabilizes TSC2 by inhibiting the interaction between TSC2 and the HERC1 ubiquitin ligase. *J. Biol. Chem.*, **281**, 8313–8316.
17. Onda, H., Lueck, A., Marks, P.W., Warren, H.B. and Kwiatkowski, D.J. (1999) Tsc2(+/−) mice develop tumors in multiple sites that express gelsolin and are influenced by genetic background. *J. Clin. Invest.*, **104**, 687–695.

18. Lan, Z.J., Xu, X. and Cooney, A.J. (2004) Differential oocyte-specific expression of Cre recombinase activity in GDF-9-iCre, Zp3cre, and Msx2Cre transgenic mice. *Biol. Reprod.*, **71**, 1469–1474.

19. Bristol-Gould, S.K., Kreeger, P.K., Selkirk, C.G., Kilen, S.M., Mayo, K.E., Shea, L.D. and Woodruff, T.K. (2006) Fate of the initial follicle pool: empirical and mathematical evidence supporting its sufficiency for adult fertility. *Dev. Biol.*, **298**, 149–154.

20. Faddy, M.J., Telfer, E. and Gosden, R.G. (1987) The kinetics of pre-antral follicle development in ovaries of CBA/Ca mice during the first 14 weeks of life. *Cell Tissue Kinet.*, **20**, 551–560.

21. Jacinto, E., Loewith, R., Schmidt, A., Lin, S., Ruegg, M.A., Hall, A. and Hall, M.N. (2004) Mammalian TOR complex 2 controls the actin cytoskeleton and is rapamycin insensitive. *Nat. Cell Biol.*, **6**, 1122–1128.

22. Sarbassov, D.D., Ali, S.M., Kim, D.H., Guertin, D.A., Latek, R.R., Erdjument-Bromage, H., Tempst, P. and Sabatini, D.M. (2004) Rictor, a novel binding partner of mTOR, defines a rapamycin-insensitive and raptor-independent pathway that regulates the cytoskeleton. *Curr. Biol.*, **14**, 1296–1302.

23. Kim, D.H., Sarbassov, D.D., Ali, S.M., King, J.E., Latek, R.R., Erdjument-Bromage, H., Tempst, P. and Sabatini, D.M. (2002) mTOR interacts with raptor to form a nutrient-sensitive complex that signals to the cell growth machinery. *Cell*, **110**, 163–175.

24. Fingar, D.C. and Blenis, J. (2004) Target of rapamycin (TOR): an integrator of nutrient and growth factor signals and coordinator of cell growth and cell cycle progression. *Oncogene*, **23**, 3151–3171.

25. Inoki, K., Corradetti, M.N. and Guan, K.L. (2005) Dysregulation of the TSC-mTOR pathway in human disease. *Nat. Genet.*, **37**, 19–24.

26. Raught, B., Peiretti, F., Gingras, A.C., Livingstone, M., Shahbazian, D., Mayeur, G.L., Polakiewicz, R.D., Sonenberg, N. and Hershey, J.W. (2004) Phosphorylation of eucaryotic translation initiation factor 4B Ser422 is modulated by S6 kinases. *EMBO J.*, **23**, 1761–1769.

27. Duncan, R. and McConkey, E.H. (1982) Preferential utilization of phosphorylated 40-S ribosomal subunits during initiation complex formation. *Eur. J. Biochem.*, **123**, 535–538.

28. Gingras, A.C., Raught, B. and Sonenberg, N. (2004) mTOR signaling to translation. *Curr. Top. Microbiol. Immunol.*, **279**, 169–197.

29. Mora, A., Komander, D., van Aalten, D.M. and Alessi, D.R. (2004) PDK1, the master regulator of AGC kinase signal transduction. *Semin. Cell Dev. Biol.*, **15**, 161–170.

30. Adhikari, D., Flohr, G., Gorre, N., Shen, Y., Yang, H.R., Lundin, E., Lan, Z.J. and Liu, K. (2009) Disruption of *Tsc2* in oocytes leads to overactivation of the entire pool of primordial follicles. *Mol. Hum. Reprod.*, **15**, 765–770.

31. Wandji, S.A., Srsen, V., Voss, A.K., Eppig, J.J. and Fortune, J.E. (1996) Initiation in vitro of growth of bovine primordial follicles. *Biol. Reprod.*, **55**, 942–948.

32. Reddy, P., Zheng, W. and Liu, K. (2009) Mechanisms maintaining the dormancy and survival of mammalian primordial follicles. *Trends Endocrinol. Metab.* In press.

33. Rajareddy, S., Reddy, P., Du, C., Liu, L., Jagarlamudi, K., Tang, W., Shen, Y., Berthet, C., Peng, S.L., Kaldis, P. and Liu, K. (2007) p27kip1 (cyclin-dependent kinase inhibitor 1B) controls ovarian development by suppressing follicle endowment and activation and promoting follicle atresia in mice. *Mol. Endocrinol.*, **21**, 2189–2202.

34. Castrillon, D.H., Miao, L., Kollipara, R., Horner, J.W. and DePinho, R.A. (2003) Suppression of ovarian follicle activation in mice by the transcription factor Foxo3a. *Science*, **301**, 215–218.

35. Liu, L., Rajareddy, S., Reddy, P., Du, C., Jagarlamudi, K., Shen, Y., Gunnarsson, D., Selstam, G., Boman, K. and Liu, K. (2007) Infertility caused by retardation of follicular development in mice with oocyte-specific expression of Foxo3a. *Development*, **134**, 199–209.

36. Hashimoto, N., Kido, Y., Uchida, T., Asahara, S., Shigeyama, Y., Matsuda, T., Takeda, A., Tsuchihashi, D., Nishizawa, A., Ogawa, W. *et al.* (2006) Ablation of PDK1 in pancreatic beta cells induces diabetes as a result of loss of beta cell mass. *Nat. Genet.*, **38**, 589–593.

37. Inoue, H., Ogawa, W., Asakawa, A., Okamoto, Y., Nishizawa, A., Matsumoto, M., Teshigawara, K., Matsuki, Y., Watanabe, E., Hiramatsu, R. *et al.* (2006) Role of hepatic STAT3 in brain-insulin action on hepatic glucose production. *Cell Metab.*, **3**, 267–275.

38. Pedersen, T. and Peters, H. (1968) Proposal for a classification of oocytes and follicles in the mouse ovary. *J. Reprod. Fertil.*, **17**, 555–557.

39. Johnson, J., Canning, J., Kaneko, T., Pru, J.K. and Tilly, J.L. (2004) Germline stem cells and follicular renewal in the postnatal mammalian ovary. *Nature*, **428**, 145–150.

40. Gingras, A.C., Raught, B. and Sonenberg, N. (2001) Regulation of translation initiation by FRAP/mTOR. *Genes Dev.*, **15**, 807–826.

41. Roux, P.P., Shahbazian, D., Vu, H., Holz, M.K., Cohen, M.S., Taunton, J., Sonenberg, N. and Blenis, J. (2007) RAS/ERK signaling promotes site-specific ribosomal protein S6 phosphorylation via RSK and stimulates cap-dependent translation. *J. Biol. Chem.*, **282**, 14056–14064.

42. van Casteren, J.I., Schoonen, W.G. and Kloosterboer, H.J. (2000) Development of time-resolved immunofluorometric assays for rat follicle-stimulating hormone and luteinizing hormone and application on sera of cycling rats. *Biol. Reprod.*, **62**, 886–894.

43. Haavisto, A.M., Pettersson, K., Bergendahl, M., Perheentupa, A., Roser, J.F. and Huhtaniemi, I. (1993) A supersensitive immunofluorometric assay for rat luteinizing hormone. *Endocrinology*, **132**, 1687–1691.